Design of Stainless Steel Tubular Section Beam-Columns

Ju Chen[a], Yuner Huang[b] and Ben Young[c]

College of Civil Engineering and Architecture, Zhejiang University, Hangzhou, China[(a)]
School of Engineering, University of Edinburgh, Edinburgh, UK[(b)]
Department of Civil Engineering, The University of Hong Kong, Pokfulam Road, Hong Kong[(c)]

Abstract

A finite element analysis and design of stainless steel tubular section beam-columns is presented in this paper. The non-linear finite element model was verified against experimental results of stainless steel tubular section beam-columns and beams. In this study, square and rectangular hollow sections were investigated. It was shown that the finite element model closely predicted the ultimate loads and failure modes of the tested beam-columns and beams. Hence, the finite element model was used for an extensive parametric study. The axial compressive strengths of the beam-column specimens predicted by the finite element analysis are compared with the design strengths calculated using the American Specification for stainless steel, direct strength method for beam-columns that proposed by Rasmussen, and linear interaction equation. Reliability analysis was performed to assess the reliability of these design rules. It is shown that these design rules generally provide accurate and reliable predictions for stainless steel tubular section beam-columns. The American Specification is slightly unconservative, and the linear interaction equation with modified direct strength method proposed by Huang and Young provide the most accurate predictions with convenient calculation procedure for stainless steel tubular section beam-columns.

Keywords

Beam-columns; Direct strength method; Finite element method; Stainless steel.

1 Introduction

Stainless steel sections have been increasingly used in building construction because of their superior corrosion resistance, ease of maintenance, and pleasing appearance. Therefore, considerable research has been carried out to investigate the structural behaviour of stainless steel members. Considerable experimental and numerical investigation on stainless steel compressive members [1-11] and flexural members [3, 12-17] has been performed. However, investigations on stainless steel beam-column members subjected to combined axial compression and bending are limited. Tests on beam-column members of austenitic stainless steel (EN 1.4301) were conducted by Talja and Salmi [18] and Kouhi et al. [19] on rectangular hollow sections (RHS), Burgan et al. [20] on I-sections, and Macdonald et al. [21] on lipped channel sections. Lui et al. [22] conducted a series of tests on cold-formed duplex stainless steel square hollow sections (SHS). Huang and Young [23, 24] and Zhao et al. [25, 26] investigated the beam-column behaviour of lean duplex stainless steel SHS and RHS.

Recently, finite element analysis has been widely used to investigate the behaviour of stainless steel members [4, 11, 17, 24, 26-29]. Finite element analysis (FEA) is relatively inexpensive and time efficient compared with physical experiments, especially when a parametric study of cross-section geometries is involved. Although FEA is a useful and powerful tool for structural analysis and design, it is important to obtain an accurate and reliable finite element model (FEM) prior to a parametric study of FEA to be carried out. Therefore, one of the purposes of this study is to develop accurate finite element models for stainless steel tubular section beam-columns and beams.

The direct strength method specified in the North American Specification [30, 31] and Australian/New Zealand Standard [32] for cold-formed steel structures was developed by Schafer and Peköz [33] and Schafer [34]. It presents a competitive alternative to existing effective section methods as it obviates lengthy effective width calculations [35]. The current direct strength method specified in the North American Specification [30, 31] and Australian/New Zealand Standard [32] is applicable for determination of the nominal axial and flexural strength of cold-formed steel members only. Rasmussen [35] applied the direct strength method to plain equal angel section beam-columns. Schafer [36] has considered the direct strength method for the design of short length of lipped channel section beam-columns and accounted for local and distortional buckling. Duong and Hancock [37] applied the direct strength method to long lipped channel beam-columns with the consideration of second order bending effect.

In this study, the behaviour and design of stainless steel tubular section on duplex (EN 1.4462) and austenitic (EN 1.4301) stainless steel beam-columns and beams were investigated using finite element analysis. A finite element model is developed and validated with the beam-column tests conducted by Lui et al. [22] and beam tests conducted by Zhou and Young [12]. The beam-column strengths obtained from the finite element analysis are compared with the design strengths predicted by the American Specification (ASCE) [38] and direct strength method for beam-columns that proposed by Rasmussen [35] and Huang and Young[24].

Paper presented by Yuner Huang - Yuner.Huang@ed.ac.uk
© Chen J (Zhejiang University), Huang Y (Uni of Edinburgh) and Young B (The University of Hong Kong)

2 Summary of Test Program

2.1 Beam-column tests

A beam-column test program on stainless steel tubular section specimens has been conducted by Lui et al. [22]. The tests were performed on two square hollow sections of duplex stainless steel. The test specimens were cold-rolled from annealed flat trips. The SHS had nominal dimension of 40 by 40 mm with thickness of 2 mm and 50 by 50 mm with thickness of 1.5 mm. The specimens were supplied from the manufacturer in uncut lengths of 3400 mm, and were cut into two different lengths of 550 mm and 1100 mm. Both ends were welded to carbon steel end plates to ensure full contact between specimen and end bearings. The test series were different by their cross-section dimensions and column lengths, testing at various eccentricities between pinned ends. Table 1 shows the average measured cross-section dimensions of the test specimens using the nomenclature defined in Fig. 1. The material properties were obtained from the coupon tests conducted by Young and Lui [39], as summarised in Table 2. The initial overall and geometric imperfections of the specimens were measured by Lui et al. [22] prior to testing. The average overall minor axis flexural imperfections at mid-length were 1/939 and 1/1883 of the specimen length for Series S1L2 and S2L2 respectively. The maximum initial local geometric imperfections of the specimens were 0.113 and 0.164 mm for section S1 (40×40×2) and S2 (50×50×1.5), respectively.

2.2 Beam tests

Zhou and Young [12] performed a series of bending tests on cold-formed stainless steel square and rectangular hollow sections. The specimens were cold-rolled from austenitic stainless steel type 304, high strength austenitic (HSA) and duplex steel sheets. The stainless steel type 304 is considered as normal strength material, whereas the HSA and duplex are considered as high strength material. The specimens consisted of 15 different section sizes, having nominal thickness (t) ranging from 1.5 to 6 mm, nominal overall depth of the webs (B_w) from 40 to 200 mm, and nominal flange widths (B_f) from 40 to 150 mm. The length of the specimens was chosen such that the section moment capacity could be obtained. Table 3 shows the measured specimen dimensions for the test specimens, using the nomenclature defined in Fig. 1. The material properties obtained from the coupon tests and ultimate load of the test specimens are summarised in Table 3.

3 Development of Finite Element Model

3.1 General

In this study, two different finite element models were developed using ABAQUS [40] for stainless steel beam-columns and beams, respectively. The four-node doubly curved shell element with reduced integration and hourglass control (S4R5) was used in the both two models. The element has five degree of freedom per node. The element allows for transverse shear deformation. In order to choose the finite element mesh that provides accurate results with minimum computational time, convergence studies were conducted. It is found that a 10 mm×10 mm (length by width) ratio provides adequate accuracy in modelling the columns. The material properties and stress-strain curves obtained from the tensile coupon tests were used in the finite element model. Since the analysis of post buckling involves large inelastic strains, the nominal (engineering) stress-strain curve was converted to a true stress and logarithmic plastic strain curve. The true stress and plastic true strain are specified in ABAQUS [40].

3.2 Beam-column model

In the simulation of beam-columns, two types of analysis were performed in the finite element analysis for buckling. The first analysis is known as eigenvalue analysis that estimates the buckling modes and loads. This analysis is a linear elastic analysis performed using the (*BUCKLE) procedure available in the ABAQUS library with the load applied within the step. For practical purposes, only the lowest buckling mode predicted from the eigenvalue analysis is used. The second analysis is called load-displacement nonlinear analysis and follows the eigenvalue prediction.

The bearing plates at both ends of the beam-columns are modelled as rigid body. In general, a rigid body is a collection of nodes, element, and/or surfaces whose motion is governed by the motion of a single node, called the rigid body reference point. The relative positions of the nodes and elements that are parts of the rigid body remain constant in the simulation. Therefore, the constituent elements do not deform but can undergo large rigid body motions. Since the motion of a rigid body can be prescribed by applying boundary conditions at the rigid body reference node, the restraints were applied on the reference point of the rigid body in this study. The reference point at the loaded end was restrained against x and y directions displacement and x-axis rotation but free to rotate about the y-axis. The reference point at another end was restrained against x, y and z directions displacement and x-axis rotation but free to rotate about the y-axis. The warping at the ends of the column was restrained. The nodes other than the two ends were free to translate and rotate in any direction.

The load was applied in increments using the modified RIKS method available in the ABAQUS library. The RIKS method is generally used to predicted unstable and nonlinear collapse of a structure such as post-buckling analysis. It

© Chen J (Zhejiang University), Huang Y (Uni of Edinburgh) and Young B (The University of Hong Kong)

uses the load magnitude as an additional unknown and solves simultaneously for loads and displacements. The nonlinear geometry parameter (NLGEOM) was included to deal with the large displacement analysis. The load was applied at the reference point of the loaded end. The loading eccentricity of beam-column was modelled as the distance from the reference point to the centroid of the specimen sections.

Both initial local and overall geometric imperfections are found in the beam-columns as a result of the fabrication process. Hence, superposition of local buckling mode as well as overall buckling mode with the measured magnitudes is recommended for accurate finite element analysis. These buckling modes could be obtained by carrying eigenvalue analysis of the column with very large value of plate width-to-thickness (b/t) ratio and very small value of b/t ratio to ensure local buckling and overall buckling occur, respectively. Only the lowest buckling mode (eigenmode 1) is used in the eigenvalue analysis. Since all buckling modes predicted by ABAQUS eigenvalue analysis are generalized to 1.0, the buckling modes are factored by the measured magnitudes of the initial local and overall geometric imperfections.

3.3 Beam model

In the simulation of beams, only half of the specimen was modelled for the symmetry. The support plate was modelled as a rigid surface, whose motion is governed by the reference point. The reference point of the support plate was restrained against x, y and z directions displacement as well as y- and z- axes rotation but free to rotate about the x-axis. The loading plate was also modelled as a rigid surface. The reference point of the loading plate was restrained against x and z directions displacement as well as y- and z- axes rotation but free to move in y directions and rotate about the x-axis. The constraint between the loading/support plate and specimen was simulated using contact surface. The web stiffener plates which stiffen the section at the load and support points were simulated by increasing the approximate 70% thickness of the elements at the corresponding parts. Thus the local failure at the loading and support points was prevented. The load was applied at the reference point of the loading plate. The nonlinear geometry parameter (NLGEOM) was included to deal with the large displacement analysis.

4 Verification of Finite Element Model

4.1 Beam-columns

The stainless steel beam-columns tested by Lui et al. [22] were modelled in this study, as shown in Fig. 2. In the finite element model (FEM), the measured cross-section dimensions, material properties and initial geometric imperfections from the tests were modelled. The measured overall geometric imperfections at mid length for minor axis flexural imperfection at mid-length were 1/939 and 1/1883 of the specimen length for Series S1 and S2 respectively, as reported by Lui et al. [22]. The maximum initial local geometric imperfections of the specimens were 0.113 and 0.164 mm for Series S1 and S2 respectively [22].

The load capacity of the stainless steel tubular section beam-columns obtained from the finite element analysis are compared with the test results conducted by Lui et al. [22] in Tables 4. A maximum difference in load capacity of 5% was observed between test and numerical results for beam-column specimens of S2L1E00, S2L1E60, S2L2E25 and S2L2E60. The mean values of the load capacity ratios (N_{TEST}/N_{FEA}, $M_{end\text{-}TEST}/M_{end\text{-}FEA}$) are 0.99 with the corresponding coefficients of variation (COV) of 0.031. The comparison indicates that the load capacity of beam-column predicted by the FEA is accurate. The failure modes obtained from the test results and FEA for each specimen are also compared in Table 4. The observed failure modes included local buckling (L) and flexural buckling (F). The failure modes observed from the finite element analysis are in good agreement with those observed in the tests, except for the specimens S2L2E60. Figs. 3 and 4 show a good agreement of the load-deflection curves and load-rotation curves obtained from the test and FEA predictions for the Series S1L1, respectively. It is shown that both the load-defection and load-rotation relationships reflect good agreement between test and finite element results. Generally, it is shown that the finite element model is accurate and reliable.

4.2 Beams

The stainless steel beams tested by Zhou and Young [12] were modelled in this study, as shown in Fig. 5. The measured cross-section dimensions and material properties reported in Table 3 were incorporated in the finite element model. The ultimate moments of the stainless steel beams obtained from the finite element analysis are compared with the test results conducted by Zhou and Young [12] in Tables 5. A maximum difference in ultimate moments of 7% was observed between test and numerical results for beam specimen of N120×60×2. The mean value of the ultimate moment ratio (M_{TEST}/M_{FEA}) is 0.97 with the corresponding coefficient of variation (COV) of 0.025. The comparison indicates that the ultimate moments of beams predicted by the FEA are accurate.

5 Parametric Study

The verification showed that the finite element models reasonably accurate for predicting the strengths of stainless steel tubular section beam-columns and beams. Hence, parametric study was carried out to investigate the behaviour of stainless steel tubular section beam-columns and beams. In the parametric study, four kinds of sections, namely 100×50×2, 150×100×2, 100×100×2 and 180×180×3 having different length of 1400 and 2800 mm were studied. The cross section dimensions are shown in Table 6, using the nomenclature defined in Fig. 1. The length of bearing plates at

© Chen J (Zhejiang University), Huang Y (Uni of Edinburgh) and Young B (The University of Hong Kong)

both ends of the specimens is assumed as 40mm. Two kinds of stainless steel material, namely high strength stainless steel grade EN 1.4462 (Duplex) and normal strength stainless steel grade EN 1.4301(AISI 304), were used in the parametric study. Material tests of stainless steel EN 1.4462 and EN 1.4301 were conducted by Chen and Young [41]. The Young's modulus E = 227 GPa, 0.2% proof stress (yield strength) $f_{0.2}$ = 731 MPa and ultimate strength f_u = 870 MPa are used for high strength stainless steel grade EN 1.4462 (Duplex), while E = 187 GPa, $f_{0.2}$ = 398 MPa and f_u = 709 MPa are used for normal strength stainless steel grade EN 1.4301 (AISI 304).

Different eccentricities were considered for each specimen. The specimens are separated into eight series according to their material properties, section dimension and specimen length. The specimens are labelled such that the material properties, section dimension, specimen length and eccentricity could be identified from the label. For example, the labels "HS100×50×1400E30" define the specimens having high strength material and nominal overall depth of the web of 50 mm, overall flange width of 100 mm, and length of 1400 mm with the eccentricity of 30 mm; the labelled 'NS100×100×2800E60' defines the specimen having normal strength material and nominal overall depth of the web of 100 mm, overall flange width of 100 mm, and length of 2800 mm with eccentricity of 60 mm. The load capacities (N_{FEA}, M_{FEA}) obtained from the finite element analysis are shown in Tables 7 – 22 and Table 24.

6 Design Rules and Comparison of Design Strengths

6.1 General

In this study, the nominal strengths (unfactored design strengths) of the stainless steel beam-columns were calculated using ASCE Specification [38], direct strength method for beam-columns that proposed by Rasmussen [35], linear interaction equations with direct strength method in AISI [30, 31], and linear interaction equations with modified direct strength method proposed by Huang and Young [24]. The cross-section dimensions and material properties used in the parametric study were adopted in the calculation of design strengths. The design strengths were compared with the numerical results obtained from the parametric study, and thus the suitability of the existing design rules were assessed.

6.2 Reliability analysis

The reliability of the beam-column design rules in the ASCE Specification [38] as well as direct strength method proposed by Rasmussen [35] and Huang and Young [24] are assessed. Reliability analysis detailed in the Commentary of the ASCE Specifications [38] is used in this study. A target reliability index of 2.5 for stainless steel structural members is used as a lower limit in this study. The design rules are considered to be reliable if the reliability index is greater than or equal to the target value. The resistance factors (ϕ) of 0.85 and 0.90 were used in calculating the reliability index (β) of axial strength and moment capacity, respectively. The load combinations of 1.2DL+1.6LL specified in ASCE [38] is adopted, where DL is the dead load and LL is the live load. The mean value (P_m) and coefficient of variation (V_p) of tests and FEA to the design predictions ratio are shown in Tables 7 – 24. In calculating the reliability index, the correction factor (C_p) as shown in Eq. F1.1-4 of the AISI S100 Specification [30] was used to account for the influence due to a small number of data. The reliability indices for axial compressive strengths of the beam-column members are shown in Tables 7 – 23, while the reliability indices for flexural strengths are shown in Table 24.

6.3 ASCE specification

According to the ASCE Specification [38], the unfactored design axial strength N_u for beam-columns is calculated by the following interaction equations:

$$\frac{N_u}{N_c} + \frac{C_m M_{e,u}}{M_b} \le 1.0 \tag{1}$$

$$\frac{N_u}{N_s} + \frac{M_{end,u}}{M_b} \le 1.0 \tag{2}$$

$$\frac{N_u}{N_c} + \frac{M_{end,u}}{M_b} \le 1.0 \tag{3}$$

where $M_{end,u}$ is the end moment corresponding to the design strength, $M_{end,u} = N_u \times e_p$; $M_{e,u}$ is the design second-order elastic moment, $M_{e,u} = M_{end,u}/(1-N_u/N_{ey})$; N_{ey} is the elastic flexural buckling load; C_m is the coefficient for unequal end moment; N_s and N_c are the section strength and member strength in compression, respectively; and M_b is the flexural strength. In this study, the design axial strength N_u calculated by ASCE Specification is represented by N_{ASCE}.

The unfactored design strengths (N_{ASCE}) calculated using the ASCE Specification are compared with the numerical results of stainless steel tubular section beam-columns in Tables 7-22 for each Series and Table 23 for all 158 specimens. Generally, it is shown that the ASCE Specification provides slightly unconservative and scatter predictions

© Chen J (Zhejiang University), Huang Y (Uni of Edinburgh) and Young B (The University of Hong Kong)

for stainless steel tubular section beam-columns. It is observed that the FEA-to-design strength ratios (N_{FEA}/N_{ASCE}) increase with eccentricities in each Series. The ASCE Specification generally provides quite unconservative predictions for eccentrically loaded columns with eccentricity e_p = 0, with N_{FEA}/N_{ASCE} ratio smaller than 1.0. The N_{FEA}/N_{ASCE} ratios for eccentrically loaded columns are ranged from 0.69 for specimen NS150-100-2800E00 to 1.04 for specimen HS100-50-1400E00. For all 158 specimens, the mean value of the N_{FEA}/N_{ASCE} ratio is 0.99 with coefficient of variation equal to 0.108, as shown in Table 23. The reliability index (β) is larger than the target value of 2.5.

The unfactored design flexural strengths (M_b) in Eqs (1)-(3) are calculated using the design rules in ASCE Specification for flexural members. In the context of this paper, it is represented by M_{ASCE}. The design flexural strengths are compared with the numerical results of stainless steel beam members of tubular section, as summarized in Table 24. It is shown that the ASCE Specification conservatively predicted the strengths of stainless steel tubular section beams. The mean value of the M_{FEA}/M_{ASCE} ratio is 1.11 with the corresponding COV of 0.055 and the reliability index of 2.93.

6.4 Direct strength method for beam-columns proposed by Rasmussen [35]

Rasmussen [35] applied the direct strength method to equal angel section beam-column with locally unstable legs. The calculation for stainless steel tubular section beam-columns follows the equations proposed by Rasmussen [35]. The design axial strength for beam-column members ($N_{DSM,R}$) as shown in Eq. (4 - 7):

$$N_{DSM,R} = \frac{r_n}{\left[\left(\frac{1}{N_Y}\right)^2 + \left(\frac{e}{M_Y}\right)^2\right]^{1/2}} \tag{4}$$

$$r_n = \begin{cases} r_{ne} & \text{for} \quad \lambda_n \le 0.776 \\ \left[1 - 0.15\left(\frac{r_{cr}}{r_{ne}}\right)^{0.4}\right]\left(\frac{r_{cr}}{r_{ne}}\right)^{0.4} r_{ne} & \text{for} \quad \lambda_n > 0.776 \end{cases} \tag{5}$$

$$r_{cr} = \left[\left(\frac{N_{ocr}}{N_Y}\right)^2 + \left(\frac{M_{ocr}}{M_Y}\right)^2\right]^{1/2} \tag{6}$$

$$r_{ne} = \left[\left(\frac{N_{one}}{N_Y}\right)^2 + \left(\frac{M_{one}}{M_Y}\right)^2\right]^{1/2} \tag{7}$$

where e is the amplified eccentricity; r_n, r_{cr} and r_{ne} are calculated using Eqs (5-(7); λ_n is the beam-column slenderness; N_{ocr} and M_{ocr} are the local buckling strength for column and beam using finite strip analysis [42], respectively; N_{one} and M_{one} are the overall buckling strength for column and beam, respectively; and N_Y and M_Y are the squash load and yield moment, respectively. Detail calculation procedure can be found in Rasmussen [35]. The Eq. (4) can be also represented as Eq. (8), which is in a similar format as the direct strength equation in AISI [30, 31]:

$$N_{DSM,R} = \begin{cases} N_{one} & \text{for} \quad \lambda_n \le 0.776 \\ \left[1 - 0.15\left(\frac{N_{ocr}}{N_{one}}\right)^{0.4}\right]\left(\frac{N_{ocr}}{N_{one}}\right)^{0.4} N_{one} & \text{for} \quad \lambda_n > 0.776 \end{cases} \tag{8}$$

The unfactored design strengths ($N_{DSM,R}$) calculated using the direct strength method are compared with the numerical results of stainless steel tubular section beam-columns in Tables 7 – 22 for each Series, and Table 23 for all 158 specimens. Generally, it is shown that the direct strength method for beam-columns proposed by Rasmussen [35] accurately predicted the strengths of stainless steel tubular section beam-columns, despite the fact that Rasmussen [35] proposed for equal angel section beam-columns. The predictions are less scatter compared with the ASCE Specification. For all 158 specimens, the mean value of the $N_{FEA}/N_{DSM,R}$ ratio is 1.02 with COV of 0.094. The reliability index (β) equals to 2.72, which is higher than the target value of 2.50. Therefore, the direct strength method for beam-columns that proposed by Rasmussen [35] is considered to provide accurate and reliable predictions for the stainless steel SHS and RHS.

© Chen J (Zhejiang University), Huang Y (Uni of Edinburgh) and Young B (The University of Hong Kong)

The design beam strength is calculated by the direct strength equations specified in AISI [30, 31] Clause 1.2.2 for beam design. It is also the same as the direct strength method with linear interaction equation (1st approach) as detailed in Section 6.5. Therefore, it is represented by $M_{DSM,AISI}$ in this study. The unfactored design beam strengths ($M_{DSM,AISI}$) are compared with the numerical results of stainless steel beams, as reported in Table 24. It is shown that the existing direct strength equations in AISI [30, 31] for beam design conservatively predicted the flexural strengths of stainless steel tubular section beams, with the mean value of the $M_{FEA}/M_{DSM,AISI}$ ratio is 1.15 with the corresponding COV of 0.060. The reliability index equals to 3.06, which is higher than the target value 2.50.

6.5 e nlinear interaction equation with direct strength method

Huang and Young [24] suggested that linear interaction equation as shown in Eq. (9) is used for lean duplex stainless steel rectangular and square hollow section beam-column members, where N_n and M_n are the nominal compressive strength for compression members and nominal flexural strength for beams, respectively.

$$\frac{N_u}{N_n} + \frac{M_{e,u}}{M_n} \leq 1.0 \tag{9}$$

Therefore, linear interaction equation is adopted in this study, with two approaches to obtain the N_n and M_n in calculation. In the first approach, N_n and M_n are calculated by the existing direct strength equations in AISI [30, 31], according to Clause 1.2.1 and Clause 1.2.2 for column design and beam design, respectively. In the second approach, N_n is calculated by the modified direct strength equations proposed by Huang and Young [11], while M_n is calculated by the modified direct strength equation in Huang and Young [17]. The calculation procedure using the 2nd approach is also detailed in Huang and Young [24]. In this study, $N_{DSM,AISI}$ is used to represent the axial strength (N_u), when the N_n and M_n are obtained from the 1st approach. Similarly, $N_{DSM,H\&Y}$ is used to represent the axial strength (N_u), when the N_n and M_n are obtained from the 2nd approach.

The unfactored design strengths ($N_{DSM,AISI}$ and $N_{DSM,H\&Y}$) calculated using the direct strength method are compared with the numerical results in Tables 7 – 22 for each Series, and Table 23 for all 158 specimens. It is shown that the direct strength method using the 1st approach provides a slightly conservative prediction for the strengths of stainless steel tubular section beam-columns. The mean value of the $N_{FEA}/N_{DSM,AISI}$ ratio for all 158 specimens is 1.05 with coefficient of variation of 0.091, as shown in Table 23. On the other hand, the direct strength method using the 2nd approach accurately predicted the numerical beam-column strengths. The mean value of the $N_{FEA}/N_{DSM,H\&Y}$ ratio is 1.00 with coefficient of variation of 0.098, as shown in Table 23. The reliability indices of both methods are greater than the target value. It should be noted that the calculation procedure of the linear interaction equation is the more convenient than the design rule in ASCE Specification and the direct strength method for beam-columns proposed by Rasmussen [35]. The design rule in ASCE Specification involves iterative process, and the calculation procedure in the direct strength method for beam-columns that proposed by Rasmussen [35] involves more steps to obtain the design strength. Considering the accuracy, reliability and convenience in calculation procedure, it is recommended that the linear interaction equation with modified direct strength method proposed by Huang and Young [24] is used for stainless steel tubular section beam-columns.

The unfactored design beam strengths in the 1st approach ($M_{DSM,AISI}$) is calculated by the direct strength equations specified in AISI [30, 31] Clause 1.2.2 for beam design. The comparison of the design strengths with numerical strengths has been detailed in Section 6.4 of this paper, as the direct strength method for beam-columns proposed by Rasmussen [35] also adopts the same method in calculating the flexural strengths. The unfactored design beam strength in 2nd approach ($M_{DSM,H\&Y}$) is calculated by the modified direct strength equation in Huang and Young [17]. The comparison of the unfactored design beam strengths ($M_{DSM,H\&Y}$) with the numerical results of stainless steel beam members is summarized in Table 24. It is shown that the modified direct strength equation in Huang and Young [17] for flexural members provides slightly conservative prediction for the stainless steel tubular section beams. The mean value of the $M_{FEA}/M_{DSM,H\&Y}$ ratio is 1.08 with the corresponding COV of 0.061 and the reliability index of 2.81. It is shown that all of the design rules for flexural members are considered to be reliable. The comparison of the FEA results with the design curve obtained using the direct strength method for beam-columns proposed by Rasmussen [35] are shown in Fig. 6. It is shown that the curve obtained using the direct strength method generally follows the distribution of the FEA results.

In load-end moment interaction curve, the numerical results ($M_{end,FEA}$, N_{FEA}) can be directly compared with the design strengths ($M_{end,d}$, N_d) calculated from design specifications for each specimen, as shown in Fig. 7. The design strength ($M_{end,d}$, N_d) of a specimen is equivalent to the intersect point between the design curve and the line connecting the origin and the numerical result of that specimen. Therefore, the interaction design curves showing relationships between load and end moment (M_{end}) are compared with the numerical results for series HS100-50-1400, as shown in Fig. 8(a). The design equations in ASCE specification and the linear interaction equation, as detailed in Sections 6.3 and 6.5, indicated a linear relation between load and second-order elastic moment (M_e). Therefore, the load and second-order elastic moment (M_e) interaction curves are compared with FEA results for series HS100-50-1400 in Fig. 8(b). It is shown that the direct strength method prediction with linear interaction equation using the 2nd approach, where N_n and M_n are calculated by Huang and Young [11, 17], are slightly better compared with the aforementioned design rules.

7 Conclusions

The paper presents a finite element analysis and design of stainless steel tubular section beam-columns and beams. Finite element models including geometric and material non-linearities have been developed and verified against experimental results. The failure modes at ultimate load predicted by the finite element analysis were generally in good agreement with the failure modes observed in the tests. In addition, the load-deflection curves and load-rotation curves predicted by the finite element analysis also agree well with the test results. The finite element models provided good predictions of the experimental ultimate loads for the stainless steel tubular section beam-columns and beams. Hence, a parametric study on stainless steel tubular section specimens has been performed using the developed finite element model for beam-columns. Four kinds of sections having different length of 1400 and 2800 mm were studied, while both the high strength and normal strength stainless steel were considered.

The finite element analysis results were compared with the design strengths calculated using the ASCE Specification. Generally, it is shown that the ASCE predictions for stainless steel tubular section beam-columns are slightly unconservative. Furthermore, the direct strength method for beam-columns proposed by Rasmussen [35] and linear interaction equation with direct strength method were also used to predict the stainless steel tubular section beam-column strengths. The interaction of local and overall buckling was also considered for beam-columns. The direct strength method generally provide accurate predictions for stainless steel tubular section beam-columns. Both the ASCE Specification and direct strength method conservatively predicted the stainless steel tubular section beams. Considering the accuracy, reliability and convenience in calculation procedure, it is recommended that the linear interaction equation with modified direct strength method proposed by Huang and Young [24] is used for stainless steel SHS and RHS beam-columns.

8 Figures

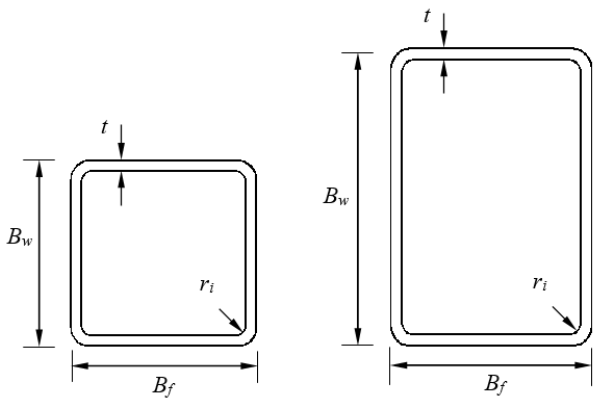

Fig. 1 Definition of symbols

© Chen J (Zhejiang University), Huang Y (Uni of Edinburgh) and Young B (The University of Hong Kong)

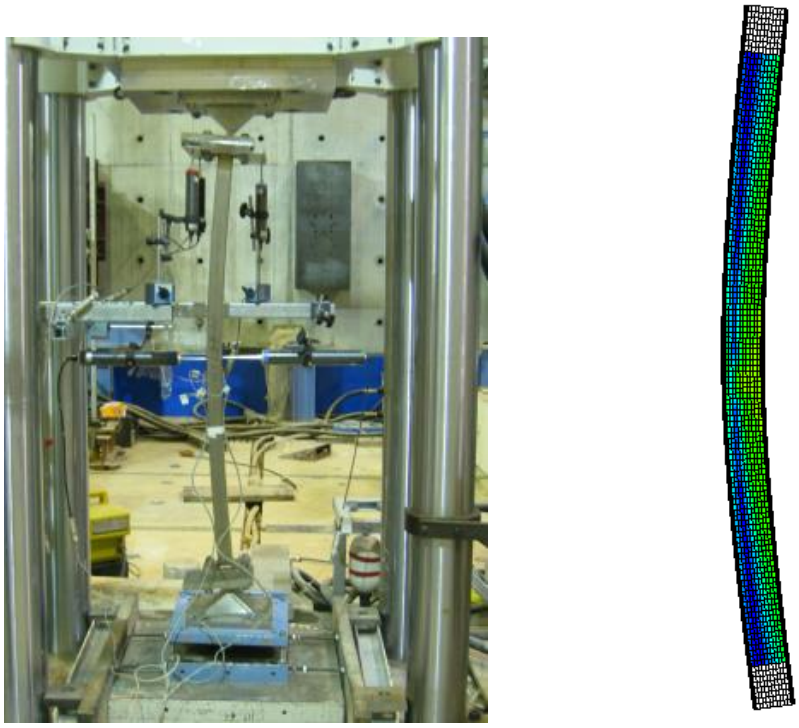

Fig. 2 Comparison of experimental and FEA deformed shapes for specimen S1L2E10

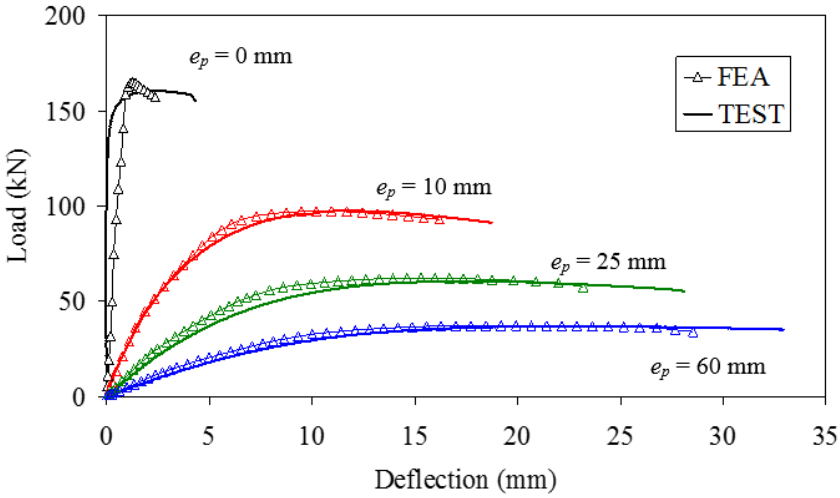

Fig. 3 Load-deflection curves for Series S1L1

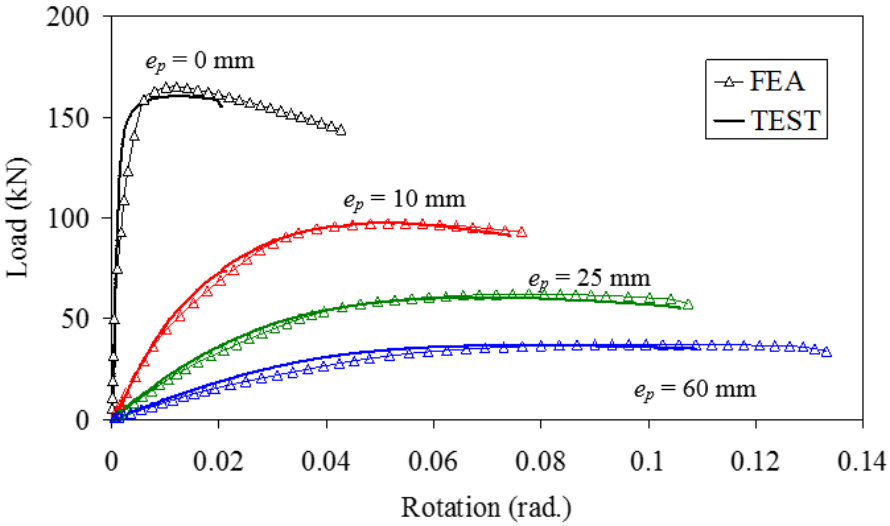

© Chen J (Zhejiang University), Huang Y (Uni of Edinburgh) and Young B (The University of Hong Kong)

Fig. 4 Load-rotation curves for Series S1L1

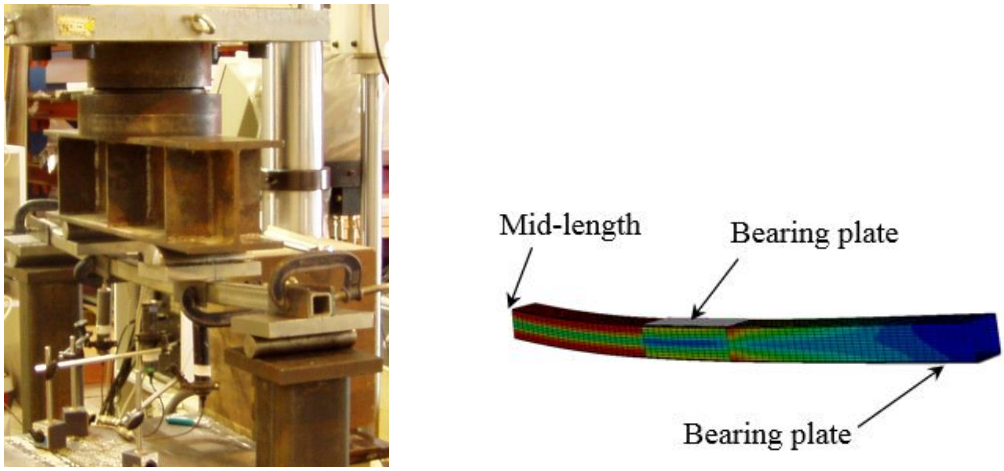

Fig. 5 Comparison of experimental specimen and FEA model for beam specimen N40×40×2

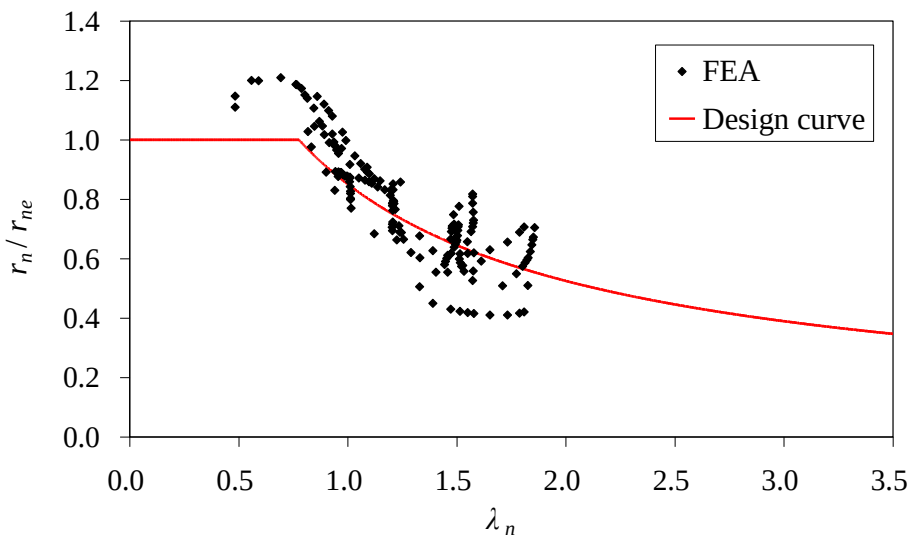

Fig. 6 Comparison of FEA results with local buckling curve using direct strength method for beam-columns proposed by Rasmussen [35]

© Chen J (Zhejiang University), Huang Y (Uni of Edinburgh) and Young B (The University of Hong Kong)

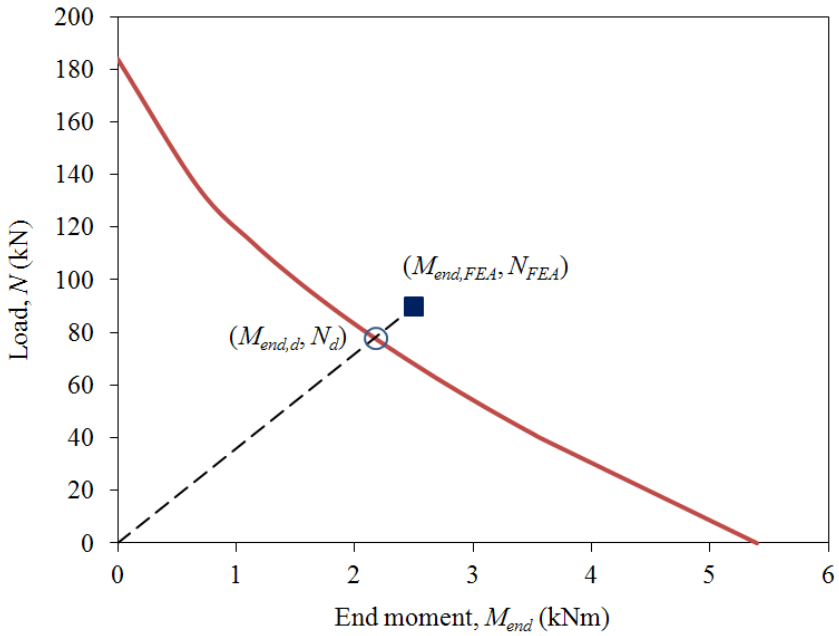

Fig. 7 Direct comparison between FEA predictions and design predictions in load-end moment diagram

© Chen J (Zhejiang University), Huang Y (Uni of Edinburgh) and Young B (The University of Hong Kong)

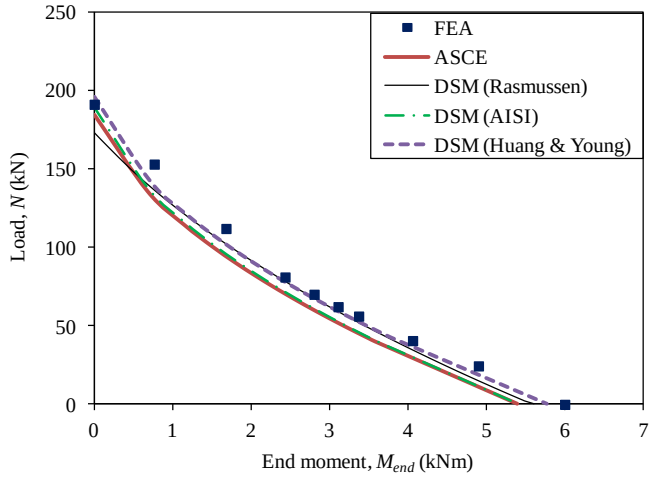

(a) Load and end moment relationship

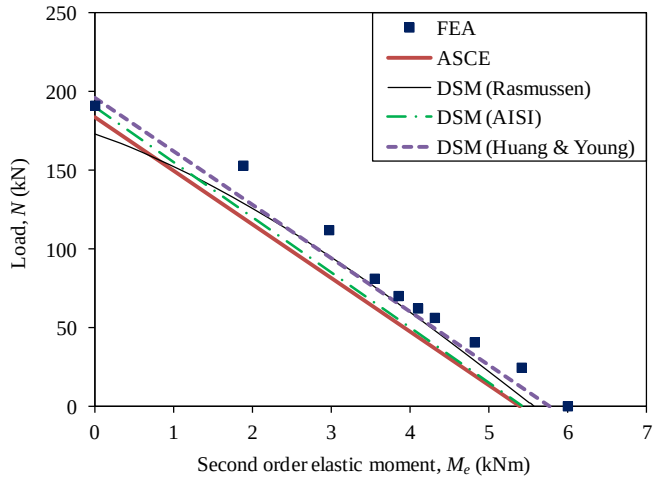

(b) Load and second order elastic moment relationship

Fig. 8 Comparison of FEA results with design curves for Series HS100-50-1400

9 Tables

Table 1 Mean value of stainless steel beam-column specimen dimensions (Lui et al. [22])

Specimen	Dimension (mm)					
	B_w	B_f	t	r_i	L	l_e
S1L1	40.2	39.9	1.919	2.3	550	630
S1L2	40.2	40.0	1.954	2.3	1100	1180
S2L1	50.2	50.1	1.538	2.3	550	630
S2L2	50.1	50.0	1.534	2.3	1100	1180

Table 2 Material properties of stainless steel specimens (Young and Lui [39])

Series	Flat portion			Corner portion		
	E (GPa)	$f_{0.2}$ (MPa)	f_u (MPa)	E (GPa)	$f_{0.2}$ (MPa)	f_u (MPa)
S1	216	707	827	214	880	1170
S2	200	622	770	214	774	1029

© Chen J (Zhejiang University), Huang Y (Uni of Edinburgh) and Young B (The University of Hong Kong)

Table 3 Dimension of stainless steel beam specimens and test results (Zhou and Young [12])

Specimen	Dimension					Material properties			Test
	B_w (mm)	B_f (mm)	t (mm)	r_i (mm)	L (mm)	E (GPa)	$f_{0.2}$ (MPa)	f_u (MPa)	M_{TEST} (kNm)
N40×40×2	40.1	40.1	1.957	2.0	1442	194	447	704	2.35
N40×40×4	40.1	40.0	3.883	4.0	1441	196	565	725	5.11
N80×80×2	80.4	80.5	1.908	4.0	1442	201	398	608	6.64
N80×80×5	79.8	79.9	4.772	7.5	1443	194	448	618	24.78
N100×50×2	99.9	49.8	1.970	2.0	1440	198	320	635	8.81
N100×50×4	99.7	49.6	3.881	4.0	1439	195	378	603	21.28
N120×60×2	120.2	59.9	1.838	2.5	1442	200	361	646	10.25
N120×60×4	120.0	59.7	3.885	5.5	1442	200	392	696	34.09
H40×40×2	40.0	40.2	1.937	2.0	1243	216	707	827	3.45
H50×50×1.5	50.3	50.1	1.541	1.5	1242	200	622	770	3.48
H150×150×3	150.7	150.6	2.779	4.8	1640	189	448	699	31.68
H150×150×6	150.5	150.7	5.870	6.0	1650	194	497	761	108.60
H140×80×3	140.3	80.5	3.094	6.5	1440	212	486	736	33.97
H160×80×3	160.6	80.9	2.901	6.0	1440	208	536	766	39.36
H200×110×4	197.7	109.1	3.998	8.5	1644	200	503	961	80.15

Table 4 Comparison of FEA results with beam-column test results obtained by Lui et al. [22]

Specimen	Test			FEA			Comparison
	Failure mode	N_{TEST} (kN)	$M_{end-TEST}$ (kNm)	Failure mode	N_{FEA} (kN)	$M_{end-FEA}$ (kNm)	$\frac{N_{TEST}}{N_{FEA}}, \frac{M_{end-TEST}}{M_{end-FEA}}$
S1L1E00	F	160.6	0.00	F	165.1	0.00	0.97
S1L1E10	F	97.5	0.98	F	97.3	0.97	1.00
S1L1E25	F	60.6	1.52	F	62.2	1.56	0.97
S1L1E60	F	36.9	2.21	F	37.3	2.24	0.99
S1L2E00	F	76.8	0.00	F	77.8	0.00	0.99
S1L2E10	F	56.9	0.57	F	55.8	0.56	1.02
S1L2E25	F	39.5	0.99	F	40.7	1.02	0.97
S1L2E60	F	25.6	1.54	F	26.4	1.58	0.97
S2L1E00	L+F	157.6	0.00	L+F	166.3	0.00	0.95
S2L1E10	L+F	104.8	1.05	L+F	100.9	1.01	1.04
S2L1E25	L+F	66.9	1.67	L+F	67.6	1.69	0.99
S2L1E60	L+F	40.6	2.44	L+F	38.7	2.32	1.05
S2L2E10	F	70.7	0.71	F	70.3	0.71	1.01
S2L2E25	F	50.0	1.25	F	52.5	1.31	0.95
S2L2E60	L+F	31.2	1.87	F	32.9	1.97	0.95
			Mean				0.99
			COV				0.031

© Chen J (Zhejiang University), Huang Y (Uni of Edinburgh) and Young B (The University of Hong Kong)

Table 5 Comparison of FEA results with beam test results obtained by Zhou and Young [12]

Specimen	MTEST (kNm)	MFEA (kNm)	MTEST / MFEA
N40×40×2	2.35	2.42	0.97
N40×40×4	5.11	5.37	0.95
N80×80×2	6.64	6.94	0.96
N80×80×5	24.78	24.89	1.00
N100×50×2	8.81	9.19	0.96
N100×50×4	21.28	22.73	0.94
N120×60×2	10.25	11.03	0.93
N120×60×4	34.09	33.63	1.01
H40×40×2	3.45	3.45	1.00
H50×50×1.5	3.48	3.62	0.96
H150×150×3	31.68	32.85	0.96
H150×150×6	108.60	111.38	0.98
H140×80×3	33.97	35.80	0.95
H160×80×3	39.36	41.07	0.96
H200×110×4	80.15	80.20	1.00
		Mean	0.97
		COV	0.025

Table 6 Dimension of stainless steel SHS and RHS specimens in parametric study

Specimen	Dimension					
	B_w (mm)	B_f (mm)	t (mm)	r_i (mm)	L (mm)	l_e (mm)
100-50-1400	50	100	2.0	2.3	1400	1480
100-50-2800	50	100	2.0	2.3	2800	2880
150-100-1400	100	150	2.0	2.3	1400	1480
150-100-2800	100	150	2.0	2.3	2800	2880
100-100-1400	100	100	2.0	2.3	1400	1480
100-100-2800	100	100	2.0	2.3	2800	2880
180-180-1400	180	180	3.0	5.3	1400	1480
180-180-2800	180	180	3.0	5.3	2800	2880

Table 7 Comparison of FEA results with design strengths of Series HS100-50-1400

Specimen	N_{FEA} (kN)	$\frac{N_{FEA}}{N_{DSM,R}}$	$\frac{N_{FEA}}{N_{DSM,AISI}}$	$\frac{N_{FEA}}{N_{DSM,H\&Y}}$	$\frac{N_{FEA}}{N_{ASCE}}$
HS100-50-1400E00	191.1	1.10	1.01	0.98	1.04
HS100-50-1400E05	153.0	1.10	1.11	1.08	1.13
HS100-50-1400E15	112.0	1.06	1.10	1.06	1.12
HS100-50-1400E30	81.1	1.02	1.06	1.02	1.08
HS100-50-1400E40	70.1	1.02	1.06	1.02	1.08
HS100-50-1400E50	62.2	1.02	1.07	1.02	1.08
HS100-50-1400E60	56.2	1.03	1.08	1.03	1.09
HS100-50-1400E100	40.6	1.05	1.09	1.04	1.10
HS100-50-1400E200	24.5	1.08	1.12	1.06	1.12
Mean (P_m)		1.05	1.08	1.03	1.09
COV(V_P)		0.032	0.031	0.029	0.025
Resistance factor (ϕ)		0.85	0.85	0.85	0.85
Reliability index (β)		3.03	3.13	2.96	3.20

© Chen J (Zhejiang University), Huang Y (Uni of Edinburgh) and Young B (The University of Hong Kong)

Table 8 Comparison of FEA results with design strengths of Series HS100-50-2800

Specimen	N_{FEA} (kN)	$\frac{N_{FEA}}{N_{DSM,R}}$	$\frac{N_{FEA}}{N_{DSM,AISI}}$	$\frac{N_{FEA}}{N_{DSM,H\&Y}}$	$\frac{N_{FEA}}{N_{ASCE}}$
HS100-50-2800E00	68.4	1.15	1.15	1.15	1.01
HS100-50-2800E05	61.5	1.20	1.24	1.23	1.16
HS100-50-2800E15	52.6	1.19	1.26	1.24	1.19
HS100-50-2800E30	43.9	1.14	1.24	1.22	1.18
HS100-50-2800E40	39.9	1.12	1.23	1.21	1.17
HS100-50-2800E50	36.6	1.10	1.22	1.19	1.17
HS100-50-2800E60	33.9	1.08	1.21	1.18	1.16
HS100-50-2800E100	26.6	1.03	1.18	1.15	1.14
HS100-50-2800E200	17.8	1.03	1.15	1.11	1.12
HS100-50-2800E400	11.2	1.07	1.15	1.10	1.14
Mean (P_m)		1.11	1.20	1.18	1.14
COV(V_P)		0.054	0.035	0.043	0.045
Resistance factor (ϕ)		0.85	0.85	0.85	0.85
Reliability index (β)		3.18	3.57	3.45	3.33

Table 9 Comparison of FEA results with design strengths of Series HS150-100-1400

Specimen	N_{FEA} (kN)	$\frac{N_{FEA}}{N_{DSM,R}}$	$\frac{N_{FEA}}{N_{DSM,AISI}}$	$\frac{N_{FEA}}{N_{DSM,H\&Y}}$	$\frac{N_{FEA}}{N_{ASCE}}$
HS150-100-1400E00	305.3	0.91	0.92	0.86	0.82
HS150-100-1400E15	231.5	0.95	0.99	0.93	0.90
HS150-100-1400E30	189.8	1.00	1.04	0.98	0.94
HS150-100-1400E40	170.1	1.02	1.07	1.00	0.96
HS150-100-1400E50	154.0	1.04	1.08	1.02	0.98
HS150-100-1400E60	140.8	1.05	1.10	1.03	0.99
HS150-100-1400E100	105.2	1.10	1.14	1.07	1.02
HS150-100-1400E200	64.8	1.15	1.18	1.12	1.06
HS150-100-1400E400	36.8	1.19	1.22	1.15	1.09
HS150-100-1400E600	25.7	1.20	1.23	1.16	1.10
Mean (P_m)		1.06	1.10	1.03	0.99
COV(V_P)		0.093	0.091	0.092	0.088
Resistance factor (ϕ)		0.85	0.85	0.85	0.85
Reliability index (β)		2.81	2.95	2.71	2.55

© Chen J (Zhejiang University), Huang Y (Uni of Edinburgh) and Young B (The University of Hong Kong)

Table 10 Comparison of FEA results with design strengths of Series HS150-100-2800

Specimen	N_{FEA} (kN)	$\frac{N_{FEA}}{N_{DSM,R}}$	$\frac{N_{FEA}}{N_{DSM,AISI}}$	$\frac{N_{FEA}}{N_{DSM,H\&Y}}$	$\frac{N_{FEA}}{N_{ASCE}}$
HS150-100-2800E00	214.9	0.97	0.88	0.84	0.87
HS150-100-2800E15	164.6	0.92	0.96	0.93	0.93
HS150-100-2800E30	137.9	0.93	1.00	0.96	0.96
HS150-100-2800E40	125.4	0.94	1.02	0.98	0.97
HS150-100-2800E50	115.3	0.96	1.04	0.99	0.98
HS150-100-2800E60	106.9	0.97	1.05	1.00	0.99
HS150-100-2800E100	83.3	1.02	1.08	1.03	1.01
HS150-100-2800E200	54.8	1.09	1.13	1.07	1.04
HS150-100-2800E400	33.1	1.17	1.18	1.12	1.07
HS150-100-2800E600	23.9	1.21	1.21	1.14	1.09
Mean (P_m)		1.02	1.05	1.01	0.99
COV(V_P)		0.103	0.094	0.089	0.066
Resistance factor (ϕ)		0.85	0.85	0.85	0.85
Reliability index (β)		2.60	2.78	2.62	2.67

Table 11 Comparison of FEA results with design strengths of Series HS100-100-1400

Specimen	N_{FEA} (kN)	$\frac{N_{FEA}}{N_{DSM,R}}$	$\frac{N_{FEA}}{N_{DSM,AISI}}$	$\frac{N_{FEA}}{N_{DSM,H\&Y}}$	$\frac{N_{FEA}}{N_{ASCE}}$
HS100-100-1400E00	276.4	0.97	0.85	0.79	0.77
HS100-100-1400E15	208.9	1.03	0.94	0.88	0.86
HS100-100-1400E30	170.0	1.08	0.99	0.92	0.91
HS100-100-1400E40	151.8	1.11	1.01	0.94	0.93
HS100-100-1400E50	137.2	1.13	1.02	0.96	0.94
HS100-100-1400E60	125.2	1.14	1.03	0.97	0.95
HS100-100-1400E100	93.1	1.19	1.07	1.00	0.99
HS100-100-1400E200	57.1	1.25	1.10	1.04	1.02
HS100-100-1400E400	32.3	1.29	1.13	1.06	1.05
HS100-100-1400E600	22.5	1.30	1.14	1.07	1.06
Mean (P_m)		1.15	1.03	0.96	0.95
COV(V_P)		0.096	0.085	0.087	0.094
Resistance factor (ϕ)		0.85	0.85	0.85	0.85
Reliability index (β)		3.09	2.73	2.47	2.38

© Chen J (Zhejiang University), Huang Y (Uni of Edinburgh) and Young B (The University of Hong Kong)

Table 12 Comparison of FEA results with design strengths of Series HS100-100-2800

Specimen	N_{FEA} (kN)	$\frac{N_{FEA}}{N_{DSM,R}}$	$\frac{N_{FEA}}{N_{DSM,AISI}}$	$\frac{N_{FEA}}{N_{DSM,H\&Y}}$	$\frac{N_{FEA}}{N_{ASCE}}$
HS100-100-2800E00	210.0	1.00	0.92	0.90	0.93
HS100-100-2800E15	152.4	0.96	1.00	0.97	0.99
HS100-100-2800E30	125.2	0.96	1.02	0.98	0.99
HS100-100-2800E40	113.0	0.97	1.02	0.99	1.00
HS100-100-2800E50	103.3	0.97	1.03	0.99	1.00
HS100-100-2800E60	95.3	0.98	1.03	1.00	1.00
HS100-100-2800E100	73.7	1.00	1.05	1.01	1.01
HS100-100-2800E200	48.2	1.03	1.08	1.03	1.03
HS100-100-2800E400	29.0	1.07	1.11	1.05	1.04
HS100-100-2800E600	20.8	1.09	1.12	1.06	1.05
Mean (P_m)		1.00	1.04	1.00	1.00
COV(V_P)		0.046	0.055	0.044	0.033
Resistance factor (ϕ)		0.85	0.85	0.85	0.85
Reliability index (β)		2.78	2.90	2.78	2.83

Table 13 Comparison of FEA results with design strengths of Series HS180-180-1400

Specimen	N_{FEA} (kN)	$\frac{N_{FEA}}{N_{DSM,R}}$	$\frac{N_{FEA}}{N_{DSM,AISI}}$	$\frac{N_{FEA}}{N_{DSM,H\&Y}}$	$\frac{N_{FEA}}{N_{ASCE}}$
HS180-180-1400E00	730.3	0.87	0.87	0.86	0.84
HS180-180-1400E15	596.8	0.84	0.89	0.86	0.84
HS180-180-1400E30	524.7	0.87	0.93	0.90	0.87
HS180-180-1400E40	485.2	0.89	0.95	0.92	0.88
HS180-180-1400E50	450.7	0.91	0.97	0.93	0.89
HS180-180-1400E60	421.8	0.93	0.98	0.95	0.90
HS180-180-1400E200	219.6	1.03	1.08	1.02	0.95
HS180-180-1400E400	130.0	1.07	1.11	1.05	0.97
HS180-180-1400E600	92.3	1.09	1.12	1.06	0.98
HS180-180-1400E800	71.6	1.10	1.13	1.07	0.98
Mean (P_m)		0.96	1.00	0.96	0.91
COV(V_P)		0.106	0.099	0.085	0.061
Resistance factor (ϕ)		0.85	0.85	0.85	0.85
Reliability index (β)		2.37	2.57	2.47	2.35

© Chen J (Zhejiang University), Huang Y (Uni of Edinburgh) and Young B (The University of Hong Kong)

Table 14 Comparison of FEA results with design strengths of Series HS180-180-2800

Specimen	NFEA (kN)	$\frac{N_{FEA}}{N_{DSM,R}}$	$\frac{N_{FEA}}{N_{DSM,AISI}}$	$\frac{N_{FEA}}{N_{DSM,H\&Y}}$	$\frac{N_{FEA}}{N_{ASCE}}$
HS180-180-2800E00	681.8	0.90	0.91	0.83	0.79
HS180-180-2800E15	531.7	0.84	0.89	0.82	0.78
HS180-180-2800E30	465.6	0.86	0.93	0.86	0.81
HS180-180-2800E40	429.2	0.87	0.94	0.88	0.82
HS180-180-2800E50	399.7	0.89	0.96	0.89	0.84
HS180-180-2800E60	374.9	0.90	0.97	0.91	0.85
HS180-180-2800E200	201.6	1.00	1.05	0.99	0.92
HS180-180-2800E400	122.5	1.04	1.09	1.02	0.94
HS180-180-2800E600	88.3	1.07	1.11	1.04	0.96
HS180-180-2800E800	69.0	1.08	1.12	1.05	0.97
Mean (Pm)		0.94	1.00	0.93	0.87
COV(VP)		0.098	0.088	0.095	0.084
Resistance factor		0.85	0.85	0.85	0.85
Reliability index		2.34	2.59	2.29	2.08

Table 15 Comparison of FEA results with design strengths of Series NS100-50-1400

Specimen	N_{FEA} (kN)	$\frac{N_{FEA}}{N_{DSM,R}}$	$\frac{N_{FEA}}{N_{DSM,AISI}}$	$\frac{N_{FEA}}{N_{DSM,H\&Y}}$	$\frac{N_{FEA}}{N_{ASCE}}$
NS100-50-1400E00	142.0	1.02	1.01	0.86	0.80
NS100-50-1400E05	109.8	1.03	1.08	0.98	0.98
NS100-50-1400E15	79.9	1.03	1.10	1.01	1.03
NS100-50-1400E30	59.8	1.06	1.12	1.03	1.08
NS100-50-1400E40	50.3	1.04	1.10	1.02	1.07
NS100-50-1400E50	43.8	1.04	1.09	1.01	1.08
NS100-50-1400E60	39.1	1.04	1.09	1.02	1.09
NS100-50-1400E100	27.4	1.05	1.09	1.02	1.11
NS100-50-1400E200	15.8	1.07	1.09	1.02	1.13
Mean (P_m)		1.05	1.09	1.00	1.03
COV(V_P)		0.017	0.028	0.051	0.094
Resistance factor (ϕ)		0.85	0.85	0.85	0.85
Reliability index (β)		3.03	3.18	2.77	2.70

© Chen J (Zhejiang University), Huang Y (Uni of Edinburgh) and Young B (The University of Hong Kong)

Table 16 Comparison of FEA results with design strengths of Series NS100-50-2800

Specimen	N_{FEA} (kN)	$\frac{N_{FEA}}{N_{DSM,R}}$	$\frac{N_{FEA}}{N_{DSM,AISI}}$	$\frac{N_{FEA}}{N_{DSM,H\&Y}}$	$\frac{N_{FEA}}{N_{ASCE}}$
NS100-50-2800E00	54.5	1.11	1.11	1.11	0.97
NS100-50-2800E05	48.4	1.20	1.22	1.21	1.16
NS100-50-2800E15	40.7	1.21	1.25	1.23	1.20
NS100-50-2800E30	33.5	1.19	1.24	1.22	1.21
NS100-50-2800E40	30.3	1.18	1.24	1.21	1.21
NS100-50-2800E50	27.4	1.15	1.22	1.19	1.20
NS100-50-2800E60	25.3	1.14	1.21	1.18	1.20
NS100-50-2800E100	19.5	1.10	1.19	1.15	1.19
NS100-50-2800E200	12.5	1.05	1.15	1.10	1.17
NS100-50-2800E400	7.4	1.06	1.12	1.07	1.15
Mean (P_m)		1.14	1.20	1.17	1.17
COV(V_P)		0.050	0.043	0.048	0.062
Resistance factor (ϕ)		0.85	0.85	0.85	0.85
Reliability index (β)		3.29	3.52	3.40	3.34

Table 17 Comparison of FEA results with design strengths of Series NS150-100-1400

Specimen	N_{FEA} (kN)	$\frac{N_{FEA}}{N_{DSM,R}}$	$\frac{N_{FEA}}{N_{DSM,AISI}}$	$\frac{N_{FEA}}{N_{DSM,H\&Y}}$	$\frac{N_{FEA}}{N_{ASCE}}$
NS150-100-1400E00	199.5	0.91	0.90	0.86	0.85
NS150-100-1400E15	149.1	0.94	0.96	0.92	0.91
NS150-100-1400E30	120.0	0.97	0.99	0.94	0.95
NS150-100-1400E40	106.6	0.99	1.01	0.96	0.96
NS150-100-1400E50	95.7	1.00	1.02	0.97	0.98
NS150-100-1400E60	87.0	1.01	1.03	0.98	0.99
NS150-100-1400E100	63.8	1.04	1.05	1.00	1.01
NS150-100-1400E200	38.5	1.07	1.08	1.02	1.04
NS150-100-1400E400	21.5	1.09	1.10	1.04	1.06
NS150-100-1400E600	15.0	1.11	1.11	1.05	1.07
Mean (P_m)		1.01	1.02	0.97	0.98
COV(V_P)		0.065	0.065	0.059	0.070
Resistance factor (ϕ)		0.85	0.85	0.85	0.85
Reliability index (β)		2.76	2.81	2.62	2.62

© Chen J (Zhejiang University), Huang Y (Uni of Edinburgh) and Young B (The University of Hong Kong)

Table 18 Comparison of FEA results with design strengths of Series NS150-100-28

Specimen	N_{FEA} (kN)	$\frac{N_{FEA}}{N_{DSM,R}}$	$\frac{N_{FEA}}{N_{DSM,AISI}}$	$\frac{N_{FEA}}{N_{DSM,H\&Y}}$	$\frac{N_{FEA}}{N_{ASCE}}$
NS150-100-2800E00	160.4	0.90	0.88	0.75	0.69
NS150-100-2800E15	118.0	0.91	0.95	0.85	0.82
NS150-100-2800E30	96.1	0.93	0.98	0.88	0.87
NS150-100-2800E40	86.1	0.94	0.99	0.90	0.89
NS150-100-2800E50	78.2	0.95	1.00	0.91	0.90
NS150-100-2800E60	71.8	0.96	1.01	0.92	0.91
NS150-100-2800E100	54.3	0.99	1.03	0.94	0.94
NS150-100-2800E200	34.3	1.03	1.05	0.98	0.99
NS150-100-2800E400	20.0	1.06	1.08	1.01	1.02
NS150-100-2800E600	14.2	1.08	1.09	1.02	1.04
Mean (P_m)		0.98	1.01	0.92	0.91
COV(V_P)		0.065	0.061	0.088	0.113
Resistance factor (ϕ)		0.85	0.85	0.85	0.85
Reliability index (β)		2.61	2.75	2.27	2.12

Table 19 Comparison of FEA results with design strengths of Series NS100-100-1400

Specimen	N_{FEA} (kN)	$\frac{N_{FEA}}{N_{DSM,R}}$	$\frac{N_{FEA}}{N_{DSM,AISI}}$	$\frac{N_{FEA}}{N_{DSM,H\&Y}}$	$\frac{N_{FEA}}{N_{ASCE}}$
NS100-100-1400E00	185.5	0.87	0.86	0.82	0.82
NS100-100-1400E15	139.8	0.90	0.94	0.90	0.92
NS100-100-1400E30	111.3	0.93	0.97	0.92	0.95
NS100-100-1400E40	97.1	0.93	0.97	0.92	0.96
NS100-100-1400E50	87.7	0.95	0.99	0.94	0.98
NS100-100-1400E60	79.4	0.96	1.00	0.94	0.98
NS100-100-1400E100	57.7	0.98	1.01	0.96	1.00
NS100-100-1400E200	34.4	1.01	1.02	0.97	1.02
NS100-100-1400E400	19.1	1.03	1.04	0.97	1.03
NS100-100-1400E600	13.2	1.03	1.04	0.98	1.04
Mean (P_m)		0.96	0.98	0.93	0.97
COV(V_P)		0.056	0.055	0.050	0.067
Resistance factor (ϕ)		0.85	0.85	0.85	0.85
Reliability index (β)		2.57	2.68	2.48	2.58

© Chen J (Zhejiang University), Huang Y (Uni of Edinburgh) and Young B (The University of Hong Kong)

Table 20 Comparison of FEA results with design strengths of Series NS100-100-2800

Specimen	N_{FEA} (kN)	$\frac{N_{FEA}}{N_{DSM,R}}$	$\frac{N_{FEA}}{N_{DSM,AISI}}$	$\frac{N_{FEA}}{N_{DSM,H\&Y}}$	$\frac{N_{FEA}}{N_{ASCE}}$
NS100-100-2800E00	158.7	0.94	0.93	0.81	0.76
NS100-100-2800E15	111.4	0.93	1.00	0.92	0.91
NS100-100-2800E30	89.3	0.93	1.01	0.93	0.93
NS100-100-2800E40	79.5	0.94	1.01	0.94	0.95
NS100-100-2800E50	71.8	0.94	1.01	0.94	0.95
NS100-100-2800E60	65.8	0.95	1.02	0.94	0.96
NS100-100-2800E100	49.2	0.96	1.02	0.95	0.98
NS100-100-2800E200	30.8	0.99	1.02	0.96	1.00
NS100-100-2800E400	17.8	1.01	1.03	0.96	1.02
NS100-100-2800E600	12.5	1.01	1.03	0.96	1.02
Mean (P_m)		0.96	1.01	0.93	0.95
COV(V_P)		0.033	0.030	0.048	0.080
Resistance factor (ϕ)		0.85	0.85	0.85	0.85
Reliability index (β)		2.64	2.85	2.47	2.44

Table 21 Comparison of FEA results with design strengths of Series NS180-180-1400

Specimen	N_{FEA} (kN)	$\frac{N_{FEA}}{N_{DSM,R}}$	$\frac{N_{FEA}}{N_{DSM,AISI}}$	$\frac{N_{FEA}}{N_{DSM,H\&Y}}$	$\frac{N_{FEA}}{N_{ASCE}}$
NS180-180-1400E00	442.4	0.82	0.81	0.80	0.81
NS180-180-1400E15	390.8	0.87	0.89	0.87	0.88
NS180-180-1400E30	346.8	0.91	0.94	0.92	0.92
NS180-180-1400E40	322.1	0.93	0.97	0.94	0.94
NS180-180-1400E50	292.6	0.93	0.96	0.93	0.94
NS180-180-1400E60	276.5	0.96	0.99	0.96	0.96
NS180-180-1400E200	137.6	1.02	1.04	0.99	0.99
NS180-180-1400E400	80.0	1.05	1.06	1.01	1.00
NS180-180-1400E600	56.3	1.06	1.07	1.01	1.01
NS180-180-1400E800	43.5	1.06	1.07	1.01	1.01
Mean (P_m)		0.96	0.98	0.94	0.95
COV(V_P)		0.088	0.087	0.071	0.068
Resistance factor (ϕ)		0.85	0.85	0.85	0.85
Reliability index (β)		2.46	2.54	2.46	2.48

© Chen J (Zhejiang University), Huang Y (Uni of Edinburgh) and Young B (The University of Hong Kong)

Table 22 Comparison of FEA results with design strengths of Series NS180-180-2800

Specimen	N_{FEA} (kN)	$\frac{N_{FEA}}{N_{DSM,R}}$	$\frac{N_{FEA}}{N_{DSM,AISI}}$	$\frac{N_{FEA}}{N_{DSM,H\&Y}}$	$\frac{N_{FEA}}{N_{ASCE}}$
NS180-180-2800E00	432.4	0.86	0.85	0.80	0.79
NS180-180-2800E15	371.8	0.89	0.92	0.87	0.86
NS180-180-2800E30	323.7	0.91	0.96	0.91	0.89
NS180-180-2800E40	296.5	0.92	0.97	0.92	0.91
NS180-180-2800E50	274.7	0.93	0.98	0.93	0.92
NS180-180-2800E60	255.3	0.94	0.99	0.94	0.93
NS180-180-2800E200	129.6	1.00	1.03	0.97	0.97
NS180-180-2800E400	76.6	1.03	1.05	0.99	0.98
NS180-180-2800E600	54.4	1.04	1.05	0.99	0.99
NS180-180-2800E800	42.2	1.05	1.06	0.99	0.99
Mean (P_m)		0.96	0.99	0.93	0.92
COV(V_P)		0.069	0.067	0.065	0.070
Resistance factor (ϕ)		0.85	0.85	0.85	0.85
Reliability index (β)		2.52	2.64	2.42	2.37

Table 23 Comparison of FEA results with design strengths for all beam-column specimens

	$\frac{N_{FEA}}{N_{DSM,R}}$	$\frac{N_{FEA}}{N_{DSM,AISI}}$	$\frac{N_{FEA}}{N_{DSM,H\&Y}}$	$\frac{N_{FEA}}{N_{ASCE}}$
Number of data	158	158	158	158
Mean (P_m)	1.02	1.05	1.00	0.99
COV(V_P)	0.094	0.091	0.098	0.108
Resistance factor (ϕ)	0.85	0.85	0.85	0.85
Reliability index (β)	2.72	2.84	2.59	2.55

Table 24 Comparison of FEA results with design strengths of stainless steel beams

Specimen	M_{FEA} (kNm)	$\frac{M_{FEA}}{M_{DSM,AISI}}$	$\frac{M_{FEA}}{M_{DSM,H\&Y}}$	$\frac{M_{FEA}}{M_{ASCE}}$
HS100-50	6.00	1.09	1.03	1.11
HS150-100	17.50	1.29	1.21	1.16
HS100-100	15.30	1.18	1.11	1.10
HS180-180	64.70	1.16	1.09	1.01
NS100-50	3.90	1.11	1.05	1.20
NS150-100	10.50	1.20	1.13	1.17
NS100-100	8.90	1.08	1.01	1.09
NS180-180	40.10	1.12	1.05	1.07
Mean (P_m)		1.15	1.08	1.11
COV(V_P)		0.060	0.061	0.055
Resistance factor (ϕ)		0.90	0.90	0.90
Reliability index (β)		3.06	2.81	2.93

© Chen J (Zhejiang University), Huang Y (Uni of Edinburgh) and Young B (The University of Hong Kong)

References

[1] Young B and Hartono W. Compression Tests of Stainless Steel Tubular Members. Journal of Structural Engineering, ASCE, 2002; 128(6): 754-761.

[2] Liu Y and Young B. Buckling of stainless steel square hollow section compression members. Journal of Constructional Steel Research, 2003; 59(2): 165-177.

[3] Gardner L and Nethercot DA. Experiments on stainless steel hollow sections — Part 2: Member behaviour of columns and beams. Journal of Constructional Steel Research, 2004; 60(9): 1319-1332.

[4] Ellobody E and Young B. Structural performance of cold-formed high strength stainless steel columns. Journal of Constructional Steel Research, 2005; 61(12): 1631-1649.

[5] Ashraf M, Gardner L and Nethercot DA. Compression strength of stainless steel cross-sections. Journal of Constructional Steel Research, 2006; 62(1-2): 105-115.

[6] Lecce M and Rasmussen KJR. Distortional Buckling of Cold-Formed Stainless Steel Sections: Experimental Investigation. Journal of Structural Engineering, ASCE, 2006; 132(4): 497-504.

[7] Young B and Lui WM. Tests of cold-formed high strength stainless steel compression members. Thin-walled structures, 2006; 44(2); 224-234.

[8] Rossi B, Jaspart JP and Rasmussen KJR. Combined distortional and overall flexural-torsional buckling of cold-formed stainless steel sections: Experimental investigations." Journal of Structural Engineering, ASCE, 2010; 136(4): 354 – 360.

[9] Rossi B, Jaspart JP and Rasmussen KJR. Combined distortional and overall flexural-torsional buckling of cold-formed stainless steel sections: Design. Journal of Structural Engineering, ASCE, 2010; 136(4): 361 – 369.

[10] Huang Y and Young B. Tests of pin-ended cold-formed lean duplex stainless steel columns. Journal of Constructional Steel Research, 2013; 82: 203 - 215.

[11] Huang Y and Young B. Structural performance of cold-formed lean duplex stainless steel columns. Thin-Walled Structures, 2014; 83: 59 – 69.

[12] Zhou F and Young B. Tests of cold-formed stainless steel tubular flexural members. Thin-walled structures, 2005; 43(9); 1325-1337.

[13] Kiymaz G. Strength and stability criteria for thin-walled stainless steel circular hollow section members under bending. Thin-Walled Structures, 2005; 43(10): 1534-1549.

[14] Real E and Mirambell E. Flexural behaviour of stainless steel beams. Engineering Structures, 2005; 27(10): 1465-1475.

[15] Gardner L, Talja A and Baddoo NR. Structural design of high-strength austenitic stainless steel. Thin-walled structures, 2006; 44(5); 517-528.

[16] Theofanous M, Chan TM and Gardner L. Flexural behaviour of stainless steel oval hollow sections. Thin-Walled Structures, 2009; 47(6-7): 776-787.

[17] Huang Y and Young B. Experimental and numerical investigation of cold-formed lean duplex stainless steel flexural members. Thin-Walled Structures, 2014; 73: 216 - 228.

[18] Talja A and Salmi P. Design of stainless steel RHS beams, columns and beam-columns. 1995, VTT Building Technology, Finland.

[19] Kouhi J, Talja A, Salmi P and Ala-Outinen T. Current R&D work on the use of stainless steel in construction in Finland. Journal of Constructional Steel Research, 2000; 54(1): 31-50.

[20] Burgan BA, Baddoo NR and Gilsenan KA. Structural design of stainless steel members – comparison between Eurocode 3, Part 1.4 and test results. Journal of Constructional Steel Research, 2000; 54(1): 51-73.

[21] Macdonald M, Rhodes J and Kotelko M. Stainless steel stub columns subject to combined bending and axial loading. Thin-Walled Structures, 2007; 45(10-11): 893-897.

[22] Lui WM, Ashraf M and Young B. Tests of cold-formed duplex stainless steel SHS beam-columns", Engineering Structures, 2014; 74: 111-121.

[23] Huang Y and Young B. Experimental investigation of cold-formed lean duplex stainless steel beam-columns. Thin-Walled Structures, 2014; 76: 105 - 117.

[24] Huang Y and Young B. Design of cold-formed lean duplex stainless steel members in combined compression and bending. Journal of Structural Engineering ASCE. 2015; 141(5):04014138.

[25] Zhao O, Rossi B, Gardner L, Young B. Behaviour of structural stainless steel cross-sections under combined loading – Part I: Experimental Study, Engineering Structures, 2015; 89: 236-246.

© Chen J (Zhejiang University), Huang Y (Uni of Edinburgh) and Young B (The University of Hong Kong)

[26] Zhao O, Rossi B, Gardner L, Young B. Behaviour of structural stainless steel cross-sections under combined loading – Part II: Numerical modelling and design approach, Engineering Structures, 2015; 89: 247-259.

[27] Rasmussen KJR, Burns T, Bezkorovainy P and Bambach MR. Numerical modelling of stainless steel plates in compression. Journal of Constructional Steel Research, 2003; 59(11): 1345-1362.

[28] Gardner L and Nethercot DA. Numerical Modelling of Stainless Steel Structural Components—A Consistent Approach. Journal of Structural Engineering, ASCE, 2004; 130(10): 1586-1601.

[29] Ashraf M, Gardner L and Nethercot DA. Finite element modelling of structural stainless steel cross-sections. Thin-walled structures, 2006; 44(10): 1048-1062.

[30] North American Specification for the design of cold-formed steel structural members. AISI S100-16, American Iron and Steel Institute and CSA Group, Washington, D.C.; 2016.

[31] Commentary on North American Specification for the Design of Cold-Formed Steel Structural Members. AISI S100-16-C, American Iron and Steel Institute; Washington, D.C.; 2016.

[32] Cold-formed steel structures. Australian/New Zealand Standard, AS/NZS 4600:2005, Standards Australia; Sydney, Australia; 2005.

[33] Schafer BW and Peköz T. Direct strength prediction of cold-formed steel members using numerical elastic buckling solutions. Proceedings of the 14th International Specialty Conference on Cold-Formed Steel Structures, University of Missouri-Rolla; 1998; 69-76.

[34] Schafer BW. Local, distortional, and Euler buckling of thin-walled columns. Journal of Structural Engineering, ASCE, 2002; 128(3); 289-299.

[35] Rasmussen KJR. Design of slender angle section beam-columns by the direct strength method. Journal of Structural Engineering, ASCE, 2006; 132(2): 204-211.

[36] Schafer BW. Advances in direct strength design of thin-walled members. Adv. struct., G. J. Hancock et al. eds. Balkema, 1, 333-339.

[37] Duong HM and Hancock GJ. Recent developments in the direct strength design of thin-walled members. Proc. Int. workshop on recent advances and future trends in thin-walled structures technology. J. Loughlan, Loughborough, Canopus; 2004. 43-62.

[38] Specification for the design of cold-formed stainless steel structural members. American Society of Civil Engineers; SEI/ASCE-8-02, Reston, Virginia; 2002.

[39] Young B and Lui WM. Behaviour of cold-formed high strength stainless steel sections. Journal of Structural Engineering, ASCE, 2005, 131: 1738-45.

[40] ABAQUS analysis user's manual. Version 6.5. ABAQUS, Inc; 2004.

[41] Chen J and Young B. Stress-strain curves for stainless steel at elevated temperatures. Engineering Structures, 2006; 28(2): 229-239.

[42] Papangelis JP and Hancock GJ. Computer analysis of thin-walled structural members. Computer and Structures, 1995; 56(1): 157-176.

© Chen J (Zhejiang University), Huang Y (Uni of Edinburgh) and Young B (The University of Hong Kong)